2013 American Control Conference (ACC)
Washington, DC, USA, June 17-19, 2013

State-of-charge (SOC) estimation based on a reduced order electrochemical thermal model and extended Kalman filter

Xueyan Li, Song-Yul Choe*

Abstract—**Accurate estimation of SOC of a battery is one of the most important issues to prevent the battery from being overcharged and undercharged. Currently, SOC is estimated using Coulomb counting or a stored set of data that includes a relationship between open circuit voltage (OCV) and SOC, where the OCV for a cell in operation is estimated based on the first or second order of electrical equivalent circuit model (EECM). The typical error percentage of those methods range 5-10% because of the integration error of the current over time and ignored effects in the EECM such as lithium ion concentrations, temperature, and other electrochemical phenomena.**

A new method for estimation of SOC is developed that uses a reduced order model (ROM) derived from a quasi-three dimensional full order physical model (FOM), and Extended Kalman filter (EKF) to minimize errors caused by inaccuracy of the ROM. Static and dynamic responses of the new approach at different charging and discharging current in a single cycle and multiple cycles are compared with those of Coulomb counting, ROM and ROM with EKF. The results show that the accomplished average error is approximately less than 4%.

Keywords: Li-polymer battery, Electro-chemical model, ROM, EKF, and SOC estimation

I. INTRODUCTION

Hybrid electric vehicles (HEV) or battery electric vehicles (BEV) are predicted to be dominant in the passenger vehicle market in following years, because of substantial reduction of fuel consumptions and emissions. The battery is a key component in the systems that saves and retrieves energy when needed. In order to ensure driving functionality of HEV and BEV, the amount of power as well as energy available in the battery should be known at any time to prevent an unnecessary overcharge or undercharge. The state of charge (SOC) of a battery is a gauge that predicts an amount of charges stored in anode electrode compared with the fuel left in a gas tank. Miscalculation of the SOC leads to overcharged or undercharged battery, which causes a high decay rate or a low utilization of the capacity. Therefore, it is very desirable to reduce the estimation errors for SOC as much as possible regardless of any variations in ambient temperature, current rate, vibration, humidity, and degradations. High temperatures, large SOC variance, and strenuous load profiles may accelerate aging. The SOC estimation algorithm must be dynamically accurate enough to handle slight variations in cell construction, operations, and attain numerical convergence as well as calculation speed.

A review on literatures recently published unveils that SOC estimation methods can be arranged into two main categories, with or without a mathematical model. The one 'without' is based on direct measurement of the current and a lookup table, including: the Coulomb counting, open circuit voltage (OCV) [1], resistance and impedance [2], and quantum magnetism [3]. Methods with a model can be arranged into four subcategories including: empirical models [4], electrical equivalent circuit models (EECM) [5], and full order (FOM) and reduced order (ROM) electrochemical models [6], [7], [8]. To be more accurate, it is commonplace to combine mathematical models with error correction techniques, such as with Kalman filter [9], adaptive extended Kalman filter [4], linear observer [10], sliding-mode observer [11], or neural network [12].

The first method is called the Coulomb counting that calculates SOC by integrating the measured current over time, resulting in units of C or Ah. The Coulomb counting has several drawbacks. The initial SOC cannot be estimated by the method unless recalling charging and discharging history data. In addition, typical errors of the current sensors worsen accuracy of the method. Moreover, the maximum capacity used for calculation of the percentage of the SOC gets less, so that the accuracy drops. Consequently, the accuracy of the method is dependent upon presence of initial SOC, maximum capacity, and treatments of the sensor errors.

The second method using the OCV is based a set of experimentally collected data at a low current rate along with resting periods. SOC is estimated using the coulomb counting process, and a corresponding SOC is linked to an OCV-the terminal voltage measured when the battery reaches an equilibrium state during the rest period. These values are stored in a lookup table and referenced during battery operation. However, challenging issue is the accurate measurement of the OCV because the measured terminal voltage is different from the OCV due to overpotentials and other voltage drops. The OCV-SOC method can predict the SOC accurately if the battery is sufficiently rested and completely relaxed, or it could be used with other SOC estimation method.

*X. Li is with Auburn University, Auburn, AL 36849 USA. (e-mail: xzl0017@tigermail.auburn.edu).
S.-Y. Choe is with Auburn University, Auburn, AL 36849 USA. (phone: 334-844-3328; e-mail: choe@auburn.edu).

A third method is based on a principle that impedance of a cell changes dependent upon charge states. The Nyquist plot of a cell measured by the Electrochemical Impedance Spectroscopy (EIS) at different SOCs is fitted to an electrical equivalent circuit model, showing that the impedances are dependent upon the SOC [2]. This related data is stored in a look-up table and used for the estimation during operations. However, due to the dependence on battery temperature, SOC, and current rates, the impedances cannot be accurately measured during charging and discharging processes.

The OCV-SOC method introduced above can be improved by an accurate prediction of the OCV during operations using a model. The model widely used is an empirical model [4] or a Randles' circuit model that can be the first [1] or second order [5]. This method allows for simple and easy implementation and possibility to combine with error correction. However, the values of circuit components of the model are not the same as states and conditions of operations change. In addition, the model does not provide physical characteristics of the battery. To better consider cell physics, such as ion concentration, overpotentials, and heat generation rates, model of high order are developed, such as single particle model [13], electrochemical model [8]. For application at various ambient temperatures of the model, thermal principles are considered in electrochemical model [6], where the principles are shown in Table I TABLE II. The governing equations are the electrochemical kinetics, the charge conservation, the mass balance conservation, the energy equation and Ohm's law. Since this physical full order model is very complex and consumes a high computational time, the model is inappropriate for use in real time applications, so a reduction of the model is required. The reduction is carried out for three governing equations that describe ion concentrations in electrodes and electrolytes, and the electrochemical kinetics (the Butler-Volmer equation).

Table I. The principles of the model

Input variables	Physical Principle	Output variables
Current or voltage Ambient temperature Initial OCV	Ion concentration in electrode: Mass conservation Ion concentration in electrolyte: Ohm's law Potential in electrode: Charge conservation Potential in electrolyte: Electrochemical kinetics Heat generation: Energy equation	SOC Terminal voltage Overpotential Ion concentration in electrodes and electrolyte Heat generation rate and battery temperature

- The concentration distribution inside the electrode particle is assumed to be a polynomial function of radial position within the sphere, so the order can be reduced to 3,
- the ion concentration in electrolyte is formulated in a state space domain that is truncated and regrouped, so the order can also be reduced to 3 or so,
- the Butler-Volmer equation is linearized using the Taylor extension.

As a result, the calculation time is significantly reduced while maintaining model accuracy.

However, the model cannot represent the response of the battery perfectly. These model errors can be minimized by error correction techniques by applying advanced control theory. For the battery system with current as input and terminal voltage as output, SOC is defined as a state which should be estimated. When a current is applied to the battery, the terminal voltage is compared with that of the model and the difference is then feed-backed to the model. The feedback gain is optimized with respect to dynamics and suppression of noises using EKF. In the paper, SOC estimation based on the ROM along with EKF is presented, which includes derivation of a model for determination of the EKF algorithm, experimental validations and analysis.

II. SOC ESTIMATION

A. *Definition of SOC*

SOC is defined as a ratio of the charge capacity in a cell ($Q_{\text{releasable}}$) to the maximum capacity ($Q_{\max}$) as follows. The SOC ranges from 0 to100%;

$$SOC(\%) = \frac{Q_{releasable}}{Q_{\max}} \cdot 100 \quad (1)$$

Given initial SOC and current profile, SOC at an instant is a difference from the initial SOC and an relative amount of charge discharged or charged that can be obtained by the integral of current over time divided by the maximum capacity as shown in (2), which is called the Coulomb counting;

$$SOC(t) = SOC(0) - \frac{\int_0^t \eta \cdot i \cdot \mathrm{d}\tau}{Q_{\max}} \times 100\% \quad (2)$$

where η is the efficiency coefficient, with typical values of 1.0 during charge and 0.98-1.0 during discharge due to possible charge losses by side reactions.

The definition of the SOC can be reformulated using the number of charges in the negative electrode and stoichiometric numbers. The releasable capacity is the difference of charges present in the negative electrode composite and the allowed minimum charge at the lowest stoichiometric number, while the maximum capacity is the difference of charges at the highest and lowest stoichiometric number;

$$\begin{aligned} Q_{releasable} &= \int_0^{L_-} \varepsilon_s \cdot F \cdot c_{s,ave} \cdot A \cdot dx - \varepsilon_s \cdot F \cdot c_{s,\max} \cdot x_0 \cdot A \cdot L_- \\ Q_{\max} &= \varepsilon_s F c_{s,\max} \cdot (x_{100} - x_0) \cdot A \cdot L_- \end{aligned} \quad (3)$$

where ε_s is the active material volume fraction, F is the Faraday's constant, A is the plate area of electrode, L_- denote the thickness of negative electrode, $c_{s,\text{ave}}$ and $c_{s,\max}$ is the volume-averaged and maximum concentrations in the solid particles, x_0 and x_{100} are the stoichiometry values at 0% and 100% SOC, respectively.

Substituting the capacity terms in (2) with (3) SOC can be expressed as a ratio of the average lithium concentration to the maximum lithium concentration in the negative electrode;

$$SOC = \left[\frac{1}{L_-} \int_0^{L_-} \frac{(C_{s,ave} - C_{s,\max} \cdot x_0)}{C_{s,\max} \cdot (x_{100} - x_0)} \cdot dx \right] \cdot 100\ \% \quad (4)$$

The equation above shows that the SOC can be estimated using an average ion concentration at given date of a battery, where the average ion concentration is derived from the ROM. In addition, an initial SOC or initial concentration distribution should be known, which is similar to the Coulomb counting. The errors caused by unknown initial values are minimized by a feedback loop (EKF) that processes the difference between the terminal voltage of the battery and the model.

B. The ROM with extended Kalman filter (EKF)

Principles of the EKF

A nonlinear system can be described using the following difference equation;

$$\begin{aligned} \mathbf{x}_k &= f(\mathbf{x}_{k-1}, \mathbf{u}_{k-1}, \mathbf{w}_{k-1}) \\ \mathbf{z}_k &= h(\mathbf{x}_k, \mathbf{v}_k) \end{aligned} \quad (5)$$

where $\mathbf{x}_k$ and $\mathbf{z}_k$ is the state and measurement of output at a time step k, for given input $\mathbf{u}_{k-1}$ and state $\mathbf{x}_{k-1}$ at the previous time step k-1. $\mathbf{w}_k$ and $\mathbf{v}_k$ represent the process noises and measurement noises, respectively. Both of the noises are assumed to be normally distributed with zero mean and constant covariance;

$$\begin{aligned} p(w) &\sim N(0, Q) \\ p(v) &\sim N(0, R) \end{aligned} \quad (6)$$

The EKF consists of three parts: initialization, time update, and measurement update as shown in TABLE II.

TABLE II. STEPS FOR EXTENDED KALMAN FILTER

Initialization:	Initial state estimation: $\hat{\mathbf{x}}_{k-1}$	(7)
	Initial error covariance : $\mathbf{P}_{k-1}$	
	Initial process noise covariance : $\mathbf{W}_k$	
	Initial measurement covariance : $\mathbf{V}_k$	
Time update:	State prediction: $\hat{\mathbf{x}}_k^- = f(\hat{\mathbf{x}}_{k-1}, \mathbf{u}_{k-1}, 0)$	(8)
	Error covariance prediction: $\mathbf{P}_k^- = \mathbf{A}_k \mathbf{P}_{k-1} \mathbf{A}_k^{\mathrm{T}} + \mathbf{W}_k \mathbf{Q}_{k-1} \mathbf{W}_k^{\mathrm{T}}$	
Measurement update:	Kalman gain: $\mathbf{K}_k = \mathbf{P}_k^- \mathbf{H}_k^{\mathrm{T}} (\mathbf{H}_k \mathbf{P}_k^- \mathbf{H}_k^{\mathrm{T}} + \mathbf{V}_k \mathbf{P}_{k-1} \mathbf{V}_k^{\mathrm{T}})^{-1}$	(9)
	State correction: $\hat{\mathbf{x}}_k = \hat{\mathbf{x}}_k^- + \mathbf{K}_k (\mathbf{z}_k - h(\hat{\mathbf{x}}_k^-, 0))$	
	Error covariance correction: $\mathbf{P}_k = (\mathbf{I} - \mathbf{K}_k \mathbf{H}_k) \mathbf{P}_k^-$	

where **A**, **W**, is the Jacobian matrix of partial derivatives of f with respect to **x** and **w** evaluated at the k-1 step. **H and V** are the Jacobian matrix of partial derivatives of h with respect to **x** and **w** evaluated at the k step.

Difference equation of the ROM

The averaged li-ion concentration in the negative electrode is defined as;

$$\overline{c_{s,ave}^-} = \frac{\sum c_{s,ave}^- \Delta L^-}{L^-} \quad (10)$$

At the same time the averaged ion concentration in solid particles $c_{s,ave}$ can be calculated as;

$$c_{s,ave} = \int_{r=0}^{R_s} \frac{3r^2}{R_s^3} c_s(r,t) dr \quad (11)$$

where R_s is the radius of electrode particles.

The domain equation for averaged concentration in solid particles is reduced to an ordinary differential equation;

$$\frac{d}{dt} c_{s,ave} + 3 \frac{j^{Li}}{R_s a_s F} = 0 \quad (12)$$

where j^{Li} is the current density, a_s is the interfacial surface area calculated from $3\,\varepsilon_s / R_s$.

The equation above is discretized in time domain and expressed in a finite difference equation as (13).

$$c_{s,ave}^k = c_{s,ave}^{k-1} - 3 \frac{j^{Li} \Delta t}{R_s a_s F} \quad (13)$$

So, the difference equation for $\overline{c_{s,ave}^-}$ can be obtained;

$$\overline{c_{s,ave}^-}^k = \overline{c_{s,ave}^-}^{k-1} - 3 \frac{\Delta t}{R_s a_s F} \frac{I}{AL^-} \quad (14)$$

On the other hand, the total number of ions present in negative and positive electrodes is constant, if there are no lithium ion losses caused by side reactions;

$$\overline{c_{s,ave}^-} \cdot \delta^- \cdot \varepsilon_s^- + \overline{c_{s,ave}^+} \cdot \delta^+ \cdot \varepsilon_s^+ \equiv n^{Li} \quad (15)$$

In addition, the terminal voltage V_t is the difference between OCV and overpotential η;

$$V_t = U_{OCV}^+(\bar{y}) - U_{OCV}^-(\bar{x}) - \eta \quad (16)$$

where $\bar{x}$ and $\bar{y}$ is the averaged stoichiometry number of all solid particles in the negative electrode and positive electrode;

$$\bar{x} = \frac{\overline{c_{s,ave}^-}}{c_{s,\max}^-}, \bar{y} = \frac{\overline{c_{s,ave}^+}}{c_{s,\max}^+} \quad (17)$$

As seen in the equation 16 and 17, the terminal voltage is a function of the averaged ion concentration in electrodes. Thus, it should be noted that the errors of voltage is directly coupled with the errors of ion concentrations. Finally, two equations (14) and (16) are derived that can be used for design of the EKF.

For EKF, the Jacobian matrices of A and H can be calculated as;

$$\mathbf{A} = \mathbf{I}$$

$$\mathbf{H} = \frac{\partial V_t}{\partial \overline{c_{s,ave}^-}} = \frac{\partial U_{OCV}^+}{\partial \bar{y}} \frac{\partial \bar{y}}{\partial \overline{c_{s,ave}^+}} \frac{\partial \overline{c_{s,ave}^+}}{\partial \overline{c_{s,ave}^-}} - \frac{\partial U_{OCV}^-}{\partial \bar{x}} \frac{\partial \bar{x}}{\partial \overline{c_{s,ave}^-}} \quad (18)$$

According to (15), the partial derivatives in (18) can be calculated;

$$\frac{\partial \overline{c_{s,ave}^{+}}}{\partial \overline{c_{s,ave}^{-}}} = -\frac{\delta^{-} \cdot \varepsilon_s^{-}}{\delta^{+} \cdot \varepsilon_s^{+}}$$
$$\frac{\partial \overline{y}}{\partial \overline{c_{s,ave}^{+}}} = \frac{1}{c_{s,\max}^{+}}, \frac{\partial \overline{x}}{\partial \overline{c_{s,ave}^{-}}} = \frac{1}{c_{s,\max}^{-}}. \quad (19)$$

Combination of (18) with (19) results in the Jacobian matrix **H** as;

$$\mathbf{H} = \frac{\partial U_{OCV}^{+}}{\partial \overline{y}} \frac{1}{c_{s,\max}^{+}} \left(-\frac{\delta^{-} \cdot \varepsilon_s^{-}}{\delta^{+} \cdot \varepsilon_s^{+}} \right) - \frac{\partial U_{OCV}^{-}}{\partial \overline{x}} \frac{1}{c_{s,\max}^{-}}. \quad (20)$$

The block diagram for estimation of SOC based on the ROM with EKF is shown in Fig. 1, where the equations used are included.

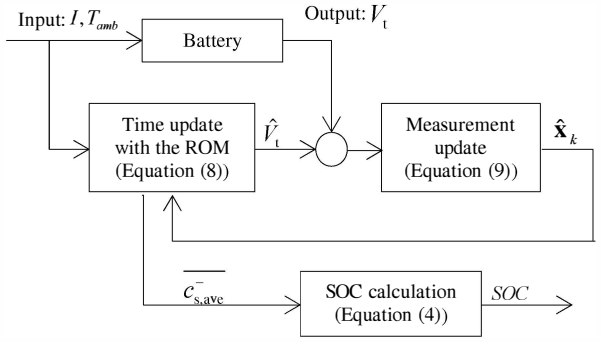

Fig. 1. Block diagram for SOC estimation based on the ROM with EKF.

C. Analysis

The designed algorithm using the ROM along with EKF for estimation of the SOC is compared with the coulomb counting and the ROM without any feedback loop, where different charging and discharging current profiles are applied as inputs. The experimental data is obtained from a test station that consists of a voltage supply and electronic load controlled by LabVIEW code embedded in a PC. Current, terminal voltage and cell temperature are measured and recorded at rates up to 100Hz. A highly accurate current sensor (0.0044% tolerance at 200A) is used for measurement of the current and estimation of the SOC using the Coulomb counting method. To minimize effects of ambient temperature on the measurement, the battery is placed vertically in a thermal chamber, where the ambient temperature is kept constant. In addition, a special clamp is also designed to reduce the contract resistance. However, there are still potential sources producing measurement errors that include nonlinear amplification factor, offsets, repeatability, to name a few. Those total errors are reflected in the simulation with an amount of 5% and white noises.

Performances of the developed method are evaluated by comparison with the experimental data (Coulomb counting) and the ROM without a feedback at different current rates and different ambient temperature for a single cycle and multiple cycles.

Static response at different current rates and different ambient temperatures

Firstly, the battery is fully discharged from the initial OCV of 4.15V with a constant current of 5C at a constant ambient temperature of 25°C. The terminal voltages and SOCs are plotted in Fig. 2 and Fig. 3, respectively, where a 0.2V OCV initial error (30% SOC error) is assumed. As expected, the ROM with EKF removes the error and follows the terminal voltage after 20 seconds. As shown in Fig. 3, the ROM can follow the experimental data when no initial errors are present, but is not able to follow the SOC once any initial error is present because of the lacking feedback loop. Overall performance of the ROM with EKF is outstanding. However, since the accuracy of EKF significantly depends on the model accuracy, there are still errors even estimated with the ROM combined with EKF.

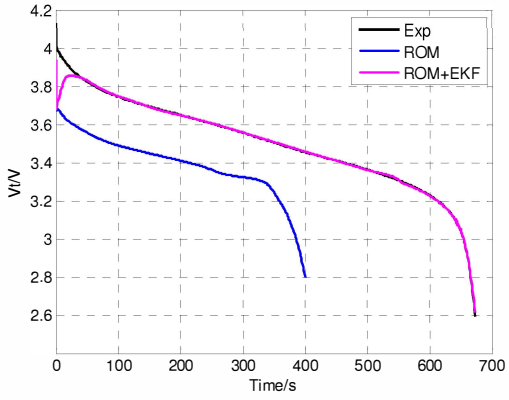

Fig. 2. Comparison between experimental and simulated terminal voltage of ROM and ROM with EKF at 5C discharge.

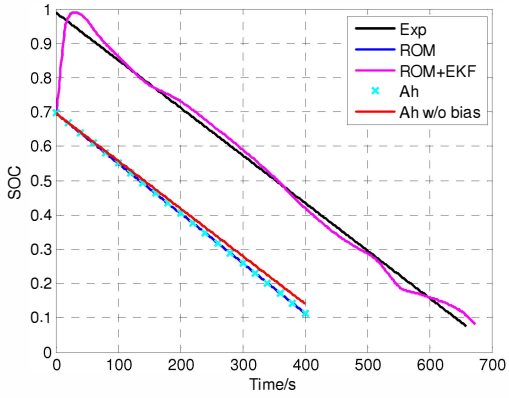

Fig. 3. Comparison between experimental and simulated SOC using three different methods at 5C discharge.

Secondly, a test is conducted to assess the responses at different ambient temperatures. The battery is placed in the thermal chamber and the ambient temperature is set to 0°C, where a current rate of 1C is applied. The terminal voltages and SOCs are plotted in Fig. 4 and Fig. 5, respectively, where an initial error of 0.2V OCV (35% SOC) is assumed.

Similar to the previous responses, the ROM with EKF works better than any others. The SOC errors become less than 5% within 20 seconds.

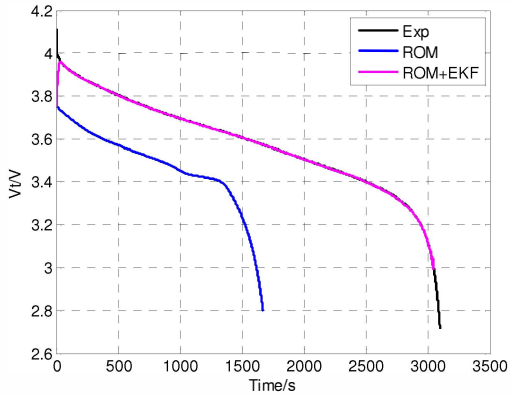

Fig. 4. Comparison of experimental and simulated terminal voltage of ROM and ROM with EKF at 1C discharge at 0°C.

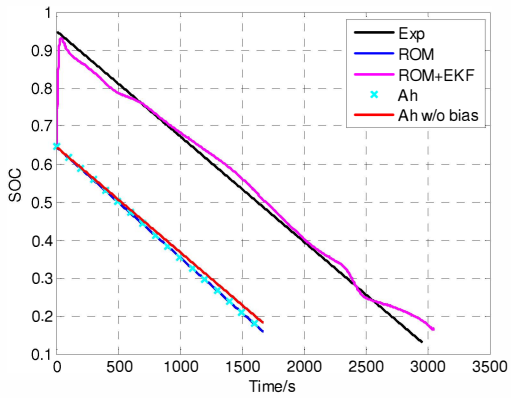

Fig. 5. Comparison of experimental and simulated SOC using three different methods at 1C discharge at 0°C.

Dynamic response

Finally, dynamic responses of the ROM with EKF are compared with those of others. In order to analyze the long term time responses, the current profile measured at BEV using a modal driving cycle - Japanese 10-15 mode, as shown in Fig. 6.

The initial OCV for the experiment and simulation is set to 4.14V and 3.94V, respectively. In addition, extra error of 5% is added to the input for the ROM to mimic the sensing errors.

The voltage and SOC responses of the current profile are shown in Fig. 7 and Fig. 8. As observed in the previous discharging behavior, the ROM with EKF is able to catch up the terminal voltage after 30 Seconds, while the ROM without the feedback cannot recognize the initial error and compensate it.

Multiple-cycle response

In addition, a current profile is created to test the numerical stability, which consists of 5 cycles with different magnitudes and periods of currents, as shown in Fig. 9. Each cycle includes a charge, a rest, a discharge, and a rest, so that all components of possible operations can be represented.

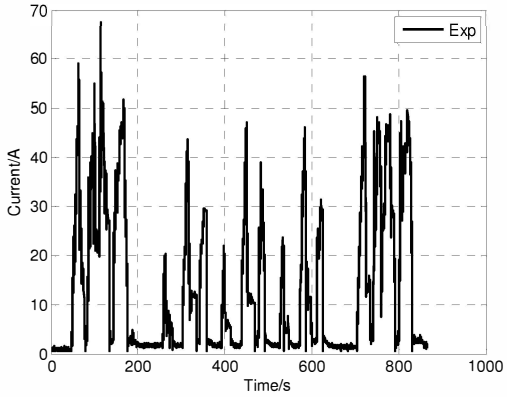

Fig. 6. Current profile of an electric vehicle measured at a driving cycle at JS10-15 mode.

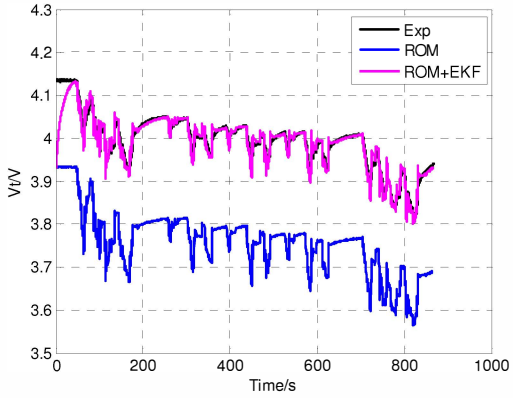

Fig. 7. Comparison between simulation results and experimental data of terminal voltage at a driving cycle.

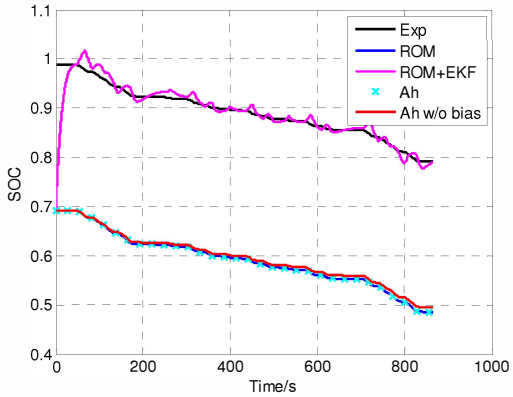

Fig. 8. Comparison of simulation results and experimental data of SOC at a driving cycle.

For analysis of effects of the sensing and initial errors, the two errors are included. The current sensing bias error is 5% and the initial error of voltage is 0.5V. The error of the SOC

estimation is plotted in Fig. 10. The Coulomb counting shows an error for the voltage that is 6.5% and relatively constant over time. In addition, the error caused by the current sensor cannot be compensated, which amounts to 5%. By contrast, the ROM with EKF shows the best tracking performance for the terminal voltage and SOC that are in a good match with the experimental data. Average errors produced under different operation conditions can be around 3%, which outperforms other methods that industry currently uses. However, there are errors at the time when a direction of the current changes, shown at the last pulse current.

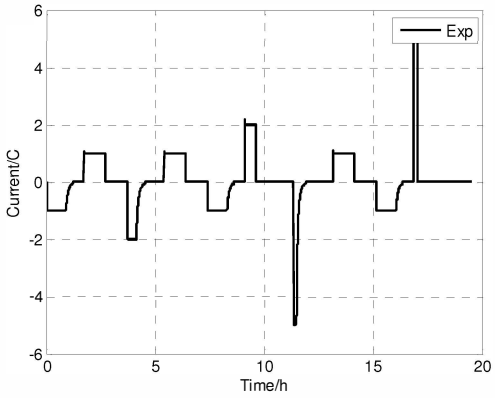

Fig. 9. Load profile for a multiple-cycle test.

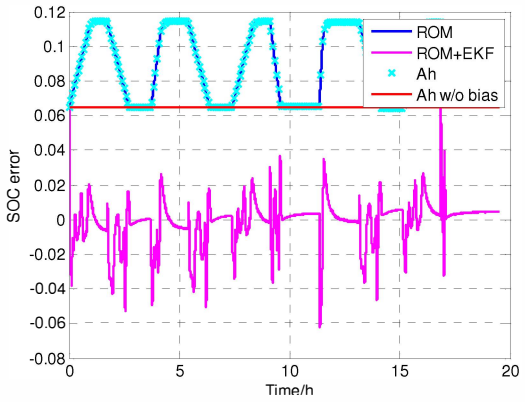

Fig. 10. Tracking behavior of three estimation methods and SOC error of ROM with EKF at a multiple-cycle test.

III. CONCLUSION

A new estimation method for SOC is proposed that is based on the ROM and EKF. The method is tested at different a single and multiple load cycles. The results of the proposing method is compared with the Coulomb counting, ROM and ROM with EKF, where effects of two typical errors are analyzed that include a current measurement error with 5% and an initial estimation error. The comparison shows that EKF based ROM significantly outperforms others with respect to not only accuracy, but also dynamics. Errors caused by models are compensated by an extra feedback loop where the terminal voltage difference between the plant and the model is used to change the averaged ion concentration of the ROM. The average estimation errors are around 4% that is less than the errors of classical methods. However, the relatively high peak of errors is produced when a pulse current is applied. The accuracy of SOC estimation could be further improved with a more accurate battery model which considers side reactions and cell aging.

REFERENCE

[1] S. Lee, J. Kim, J. Lee, and B.H. Cho, "State-of-charge and capacity estimation of lithium-ion battery using a new open-circuit voltage versus state-of-charge," J. Power Sources, Vol. 185, pp. 1367-1373, 2008.

[2] S. Rodrigues, N. Munichandraiah, and A. K. Shukla, "AC impedance and state-of-charge analysis of a sealed lithium-ion rechargeable battery," J. Solid state Electrochemistry, Vol. 3, pp. 397-405, 1999.

[3] G. P. Meisner, J. F. Herbst, and M. W. Verbrugge, "System and method to determine the state of charge of a battery using magnetostriction to detect magnetic response of battery material," U.S. Patent Application 2010/0079145, GM Global Technology Operations, Inc., April 1, 2010.

[4] F. Sun, X. Hu, Y. Zou, S, Li, "Adaptive unscented Kalman filtering for state of charge estimation of a lithium-ion battery for electric vehicles," Energy, Vol. 36, pp. 3531-3540, 2011.

[5] H. He, R. Xiong, X, Zhang, F, Sun, and J. Fan, "State-of-charge estimation of lithium-ion battery using an adaptive extended Kalman filter based on an improved Thevenin model," IEEE Transactions on Vehicular Technology, Vol. 60(4), pp. 1461-1469, 2011.

[6] M. Xiao and S.-Y. Choe, "Dynamic modeling and analysis of a pouch type LiMn2O4/Carbon high power Li-polymer battery based on electrochemical-thermal principles," J. Power Sources, Vol. 218, pp. 357-367, 2012.

[7] K. Smith, C. Rahn, and C.Y. Wang, "Control oriented 1D electrochemical model of lithium ion battery," Energy Conversion and Management, Vol. 48, 2565–2578, 2007.

[8] X. Li, M. Xiao, and S.-Y. Choe, "Reduced order of electrochemical model for a pouch type high power Li-polymer battery," International Conference on Clean Electrical Power, Ischia, Italy, June 14-16, 2011.

[9] G. L. Plett, "Extended Kalman filtering for battery management systems of LiPB-based HEV battery packs. Part 2. Modeling and identification," J. Power Sources, Vol. 134, pp. 262-276, 2004.

[10] N. A. Chaturvedi, R. Klein, J. Christensen, J. Ahmed, and A. Kojic, "Modeling, estimation, and control challenges for lithium-ion batteries," 2010 American Control Conference, Baltimore, Maryland, USA, June 30, 2010.

[11] I.-S. Kim, "Nonlinear state of charge estimator for hybrid electric vehicle battery," IEEE Transactions on Power Electronics, Vol. 23 (4), pp. 2027-2034, 2008.

[12] S. Piller, M. Perrin, and A. Jossen, "Methods for state-of-charge determination and their applications," J. of Power Sources, Vol. 96, pp. 113-120, 2001.

[13] S. Santhanagopalan, R. E. White , "Online estimation of the state of charge of a lithium ion cell," J of Power Sources, vol. 161, pp. 1346–1355, 2006